The lateral distribution of depth-averaged velocity in a channel flow bend

Tang, Xiaonan; Knight, Donald W.

DOI:
10.1016/j.jher.2014.11.004

Accepted Manuscript

The lateral distribution of depth-averaged velocity in a channel flow bend

Xiaonan Tang, Donald W. Knight

PII: S1570-6443(15)00013-1

DOI: 10.1016/j.jher.2014.11.004

Reference: JHER 311

To appear in: *Journal of Hydro-environment Research*

Received Date: 6 November 2013

Revised Date: 14 August 2014

Accepted Date: 25 November 2014

Please cite this article as: Tang, X., Knight, D.W, The lateral distribution of depth-averaged velocity in a channel flow bend, *Journal of Hydro-Environment Research* (2015), doi: 10.1016/j.jher.2014.11.004.

The lateral distribution of depth-averaged velocity in a channel flow bend

Xiaonan Tang[1] and Donald W Knight[2]

School of Civil Engineering, The University of Birmingham, Edgbaston, Birmingham B15 2TT, UK

1 – Lecturer in water engineering, 2 – Emeritus Professor

Key words: Velocity, Open channel flow, Curved channel, Channel bend, Hydraulics

Abstract

This paper proposes an analytical model to predict the lateral distribution of streamwise velocity for flow in a curved channel with vertical sides, based on the depth-integrated Navier-Stokes equations. The model includes the effects of bed friction, lateral turbulence and secondary flows, where the additional secondary flow is approximated by a linear relationship, as demonstrated by the limited data which are available. Two analytical solutions for the depth-averaged velocity are obtained, one for a flat bed and another for a bed with a transverse slope. Two parameters (denoted by *m* and *n* herein), which define the secondary flow, have been examined to analyse how they affect the velocity distribution in these two cases. Comparison of the analytical results with the limited experimental data available shows that the proposed model predicts the lateral distributions of depth-averaged velocity well. Further studies are needed to validate the values of the model parameters (*m* and *n*) for bends with different geometric properties.

The lateral distribution of depth-averaged velocity in a channel flow bend

Xiaonan Tang and Donald W Knight

School of Civil Engineering, The University of Birmingham, Edgbaston, Birmingham B15 2TT, UK

Key words: Velocity, Open channel flow, Curved channel, Channel bend, Hydraulics

Abstract

This paper proposes an analytical model to predict the lateral distribution of streamwise velocity for flow in a curved channel with vertical sides, based on the depth-integrated Navier-Stokes equations. The model includes the effects of bed friction, lateral turbulence and secondary flows, where the additional secondary flow is approximated by a linear function of the lateral distance, as demonstrated by the limited data which are available. Two analytical solutions for the depth-averaged velocity are obtained, one for a flat bed and another for a bed with a transverse slope. Two parameters (denoted by *m* and *n* herein), which define the secondary flow, have been examined to analyse how they affect the velocity distribution in these two cases. Comparison of the analytical results with the limited experimental data available shows that the proposed model predicts the lateral distributions of depth-averaged velocity well. Further studies are needed to validate the values of the model parameters (*m* and *n*) for bends with different geometric properties.

Introduction

Since the early work of Rozovskii (1957), flow in channel bends has been studied by several researchers (e.g. Engelund 1974, Ascanio and Kennedy 1983, Yalin 1992, Yeh and Kennedy 1993, Jin and Steffler 1993, Khan and Steffler 1996). Noticeable development on the knowledge and understanding of the flow structure of bend are made recently (e.g. Blanckaert & Graf, 2001, 2004; Blanckaert & de Vriend, 2003, 2005, 2010; Blanckaert *et al*. 2008; Constantinescu et al. 2011, 2013; Jamieson et al. 2010, 2013; Kashyap et al. 2012; Sukhodolov 2012, Ottevanger et al. 2013). The experimental data of velocity in a bend show two circulation cells in a cross section: alongside the classical helical motion (centre-region cell), a weaker counter-rotating cell (outer-bank cell) is formed in the corner of the outer bank near the water surface (Blanckaert & Graf, 2001). Blanckaert & Graf (2004) found the advective momentum transport by the central-region cell significantly affects the velocity profile and bed shear stress in a sharp bend, by evaluating each term of the

momentum equations using available experimental data. The cross-stream circulation in a bend was further studied by detailed 3D velocity measurements (Blanckaert *et al*. 2008; Jamieson et al. 2010, 2013). van Balen *et al*. (2009) and Stoesser et al. (2010) analyzed the pattern of secondary flow cell in a bend and its impact on the bed shear stress in terms of 3D numerical modelling, while others have developed simpler, 2D models, e.g., Hsieh and Yang (2003). With respect to 2D modelling, Blanckaert (2005) stated that "… conventional depth-averaged two dimensional (2D) models are intrinsically unable to account for the secondary flow ...". Blanckaert's statement has highlighted the need for a secondary flow correction when 2D models are applied to simulate flow in bends, particularly by supplementing the 2D models with a closure sub-model for the secondary flow.

Camporeale et al. (2007) have given a review on commonly used simple models for curved rivers to illustrate the interconnected processes among the hydrodynamics, bed morphodynamics and bank morphodynamics. Most existing hydrodynamics models for curved channel flow take account for the impact of secondary flow using a parameterization that is based on the hypothesis of mild curvature. For example, Johannesson and Parker (1989) used a perturbation expansion to linearize the depth-integration momentum equation, where the secondary flow was parameterized with an empirical shape function for the vertical distribution of primary velocity. Thus based on the linearity and gradual variation assumptions, the representation of the secondary flow is justified for small curvature channels, but it is not appropriate in moderately and strongly curved bends. For strongly curved bends, Blanckaert & De Vriend (2003, 2010) proposed a sub-model for a nonlinear treatment of the secondary flow in the depth-averaged momentum equation, where the secondary flow was parameterized through a correction factor which depends on the so-called bend parameter. Thus the derived nonlinear sub-model was a reduced-order equation. Ottevanger et al. (2013) extended the non-linear model of Blanckaert & De Vriend (2010) to the bed morphology in strongly curved bends. However, it is worth noting that all these sub-models were not directly to resolve the 2D depth-averaged momentum equations rather than they further reduced the equations by taking the average or the first moment in lateral direction.

Similar arguments have often drawn attention against quasi 2D models in straight channels, e.g., the Shiono & Knight model (SKM) (Shiono & Knight, 1991; Tang & Knight, 2008, 2009) has often been accused of being too simplistic, yet it has yielded significant insight into the flow dynamics in straight channels and has enabled reasonably accurate predictions of depth-averaged velocities, boundary shear and channel discharge to be made in natural rivers (Abril and Knight, 2004; Knight *et al*. 2007, 2010a&b; Knight 2012, Sharifi and Sterling, 2009). The aim of this paper is to illustrate that it is

possible to use the SKM to accurately predict the lateral distribution of depth-averaged velocities in bends by solving the depth-averaged momentum equation.

Before describing the mathematics relating to the SKM model it will be beneficial to outline in qualitative terms the secondary flow associated with a number of features inherent in bend flow. Since this discussion is purely qualitative, flow around a "general" bend will be discussed, as illustrated in Fig. 1. It is reasonably straightforward to demonstrate that a lateral pressure gradient exists between the inner and outer banks which are proportional to the local streamwise velocity squared and inversely proportional to the distance from the centre of curvature of the channel. Combined with the effect of boundary layer drag arising from the channel bed, the flow in a curved channel will have some relatively large scale vorticity, resulting in what is commonly termed 'Prandtl's secondary flow of the first kind' (Schlichting, 1979). Fig. 1 illustrates that the flow can be dominated by one large scale secondary flow cell which extends from the inner bank to cover most of the cross section and a corresponding small secondary flow cell near the water surface at the outer bank. This is remarkably different from what is known to exist in a straight channel where a series of secondary flow cells arise as a result of the anisotropy in Reynolds stresses (Nezu et al. 1993; Albayrak and Lemmin, 2011). Fig. 2 illustrates that at a particular cross section the flow can be conceptualised to consist of a number of different secondary flow cells which ensure that lateral gradient of $(UV)_d$ (where U represents the local streamwise velocity, V represents the local transverse velocity and the subscript d denotes a depth average) varies across the channel. A full explanation of how $(UV)_d$ is associated to the secondary cell can be seen in the paper by Knight *et al.* (2007). Subsequent sections will discuss the importance of $(UV)_d$ but for now it is sufficient to note that it can be interpreted as an indicator of the strength of secondary flow cell. Hypothesising this distribution for the case illustrated in Fig. 1 would suggest that the flow domain could be discretized into four panels – two large panels corresponding to the large secondary flow cell and smaller panels centred around the outer bend secondary flow cell. Indeed, given the relative size of the both flow cells it could be postulated that it is not unreasonably too simple to just use a two panel structure, i.e., effectively ignoring the contribution of the smaller flow cell. The feasibility of this is addressed below.

Theoretical background

The governing continuity and Reynolds Averaged Navier-Stokes equations for the streamwise motion of a fluid element in a curved channel (a cylindrical coordinate system), with a plane bed

inclined in the streamwise direction, shown in Fig.2 (a flat surface is assumed as simplicity), may be written as (Chang, 1998):

$$\frac{\partial \bar{u}}{\partial s}+\frac{\partial \bar{v}}{\partial n}+\frac{\partial \bar{w}}{\partial z}+\frac{\bar{v}}{r}=0 \quad (1)$$

$$\frac{\partial \bar{u}^2}{\partial s}+\frac{\partial(\bar{u}\,\bar{v})}{\partial n}+\frac{\partial(\bar{u}\bar{w})}{\partial z}+2\frac{\bar{u}\,\bar{v}}{r}+\left(\frac{\partial \overline{u'^2}}{\partial s}+\frac{\partial(\overline{u'v'})}{\partial n}+\frac{\partial(\overline{u'w'})}{\partial z}+2\frac{\overline{u'v'}}{r}\right)=-\frac{1}{\rho}\frac{\partial \bar{p}}{\partial s}+F_s \quad (2)$$

where the overbar and prime denote the time-averaged value and fluctuation of velocity respectively, r is a radius of the curvature, and the velocity components {u,v,w} correspond to the coordinates {s,n,z} or corresponding {x,y,z}, *s*-streamwise parallel to the channel bed, n-lateral and z-normal to the bed, ρ = fluid density, t= time, *Fs* = unit body force in the direction s, and p = pressure.

Multiplying Eq.(1) by ū and subtracting the resulting equation from (2) yields

$$\bar{u}\frac{\partial \bar{u}}{\partial s}+\bar{v}\frac{\partial \bar{u}}{\partial n}+\bar{w}\frac{\partial \bar{u}}{\partial z}+\frac{\bar{u}\,\bar{v}}{r}=-\frac{1}{\rho}\frac{\partial \bar{p}}{\partial s}+F_s-\left(\frac{\partial \overline{u'^2}}{\partial s}+\frac{\partial(\overline{u'v'})}{\partial n}+\frac{\partial(\overline{u'w'})}{\partial z}+2\frac{\overline{u'v'}}{r}\right) \quad (3)$$

When compared to a Cartesian coordinate system (x, y, z) in a straight channel, (3) has two additional terms: $\frac{\bar{u}\,\bar{v}}{r}$ on the left side and $2\frac{\overline{u'v'}}{r}$ on the right side.

For a curved open channel with a gradually varied flow along the streamwise direction, it is assumed that $F_s = 0$ (streamwise) and that $\partial p/\partial s = gS_o$, where S_o is bed slope of channel and g is acceleration of gravity. Thus Eq. (3) can be rewritten as

$$\rho\left[\frac{\partial \bar{u}^2}{\partial s}+\frac{\partial(\bar{u}\,\bar{v})}{\partial n}+\frac{\partial(\bar{u}\bar{w})}{\partial z}\right]=\rho g S_o-\rho\left[\frac{\partial \overline{u'^2}}{\partial s}+\frac{\partial(\overline{u'v'})}{\partial n}+\frac{\partial(\overline{u'w'})}{\partial z}\right]-2\rho\left(\frac{\bar{u}\,\bar{v}}{r}+\frac{\overline{u'v'}}{r}\right) \quad (4)$$

For simplicity, Eq. (4) can be written as.

$$\rho\left[\frac{\partial \bar{u}^2}{\partial s}+\frac{\partial(\bar{u}\,\bar{v})}{\partial n}+\frac{\partial(\bar{u}\bar{w})}{\partial z}\right]=\rho g S_o+\left[\frac{\partial \tau_{ss}}{\partial s}+\frac{\partial \tau_{ns}}{\partial n}+\frac{\partial \tau_{zs}}{\partial z}\right]-2\rho\left(\frac{\bar{u}\,\bar{v}}{r}+\frac{\overline{u'v'}}{r}\right) \quad (5)$$

In an open channel flow under steady flow, by depth-averaging equation (5), and noting that the velocity component of w at both the surface and the bottom of channel can be neglected, Eq.(5) becomes as:

$$\rho\left[\frac{\partial H U_d^2}{\partial s}+\frac{\partial H(\bar{u}\,\bar{v})_d}{\partial n}\right]=\rho g H S_o+\left[\frac{\partial H\overline{\tau_{ss}}}{\partial s}+\frac{\partial H\overline{\tau_{ns}}}{\partial n}\right]-2\rho\int_0^H\left(\frac{\bar{u}\,\bar{v}}{r}+\frac{\overline{u'v'}}{r}\right)dz \quad (6)$$

For a curved channel in fully developed flow conditions, where it is assumed that $\frac{\partial H U_d^2}{\partial s}\approx 0$ and $\frac{\partial H\overline{\tau_{ss}}}{\partial s}\approx 0$ in the streamwise direction at a section, Eq.(6) becomes to:

$$\rho\frac{\partial H(\bar{u}\,\bar{v})_d}{\partial n}=\rho g H S_o+\frac{\partial H\overline{\tau_{ns}}}{\partial n}-\tau_b\sqrt{1+\frac{1}{ss^2}}-2\rho\int_0^H\left(\frac{\bar{u}\,\bar{v}}{r}+\frac{\overline{u'v'}}{r}\right)dz \quad (7)$$

where the long overbar or subscript (d) denotes a depth-averaged value, τ_b is the bed shear stress, *ss* is the channel side slope of the banks (1:s*s*, vertical: horizontal), H is the flow depth, {τ_{ns} , τ_{zs} } are

Reynolds stresses on planes perpendicular to the n and *z* directions respectively, and the depth-averaged velocity U_d is defined as

$$U_d = \frac{1}{H}\int_0^H \bar{u}dz \quad (8)$$

In a Cartesian coordinate system, where {x,y,z} represent {s,n,z} respectively, as shown in Fig.2, Eq.(7) is written as

$$\rho\frac{\partial H(\bar{u}\,\bar{v})_d}{\partial y} = \rho g H S_o + \frac{\partial H\overline{\tau_{yx}}}{\partial y} - \tau_b\sqrt{1+\frac{1}{ss^2}} - 2\rho\int_0^H(\frac{\bar{u}\,\bar{v}}{r} + \frac{\overline{u'v'}}{r})dz \quad (9)$$

Eq.(9) is the depth-averaged form of the momentum equation for flow in a curved channel. In a straight channel, where the radius (r) of the curvature become infinite (∞), the last term on the RHS of Eq.(9) becomes zero, hence

$$\rho\frac{\partial H(\bar{u}\,\bar{v})_d}{\partial y} = \rho g H S_o + \frac{\partial H\overline{\tau_{yx}}}{\partial y} - \tau_b\sqrt{1+\frac{1}{ss^2}} \quad (10)$$

which is the same equation as that given by Shiono and Knight (1991). Eq.(10) also shows that the secondary flow (the term on LHS) and the last term on RHS (due to the curvature of channel) affect the flow contributing to balance the body force and Reynolds stress.

Development of a new analytical model

In a curved channel, the governing depth-averaged momentum equation (9) can be rewritten as

$$\rho g H S_o + \frac{\partial H\overline{\tau_{yx}}}{\partial y} - \tau_b\sqrt{1+\frac{1}{ss^2}} = \rho\frac{\partial H(\bar{u}\,\bar{v})_d}{\partial y} + 2\rho\int_0^H(\frac{\bar{u}\,\bar{v}}{r} + \frac{\overline{u'v'}}{r})dz \quad (11)$$

The terms on the RHS of Eq.(11) include the secondary flow term (1st term) and the contribution of additional Reynolds stress due to curvature (2nd term). Eq. (11) can apply to a straight channel where the second terms on the RHS will not exist. In a straight channel, the secondary flow term (1st term of RHS in Eq.11) is assumed to be a constant value (Γ), based on detailed measurements (Shiono and Knight, 1991). However, there are few corresponding measurements for curved channels. Hence it is not fully understood how much the additional Reynolds stress term in Eq. (11) contributes to the overall balance. Blanckaert and de Vriend (2003, 2010) proposed as a first approximation to a parabolic width distribution of the RHS terms. Similarly, as a first attempt we here assume that the overall RHS contribution varies linearly cross the channel from the centre of channel bend (see Fig. 2), and hence can be described in the form of $m + n$ y, where m and n are constants that depend on the turbulence characteristics and the geometry of the curved channel. The aim is thus to explore whether there exists any form of analytical solution for the depth-averaged velocity in a curved channel that ensures this approximate distribution of the RHS of Eq. (11). In later sections, a

preliminary analysis is made using the limited experimental data that are available, and this shows that such an approximation is reasonable and leads to useful results.

Therefore, the linear relationship between the additional flow term [RHS of Eq. (11)] and the lateral distance (y), is assumed to be given by

$$\rho \frac{\partial H(\bar{u}\,\bar{v})_d}{\partial y} + 2\rho \int_0^H \left(\frac{\bar{u}\,\bar{v}}{r} + \frac{\overline{u'v'}}{r} \right) dz = m + ny \qquad (12)$$

where *m* and *n* are constants to take into account the influence of secondary flow and the additional Reynolds stress due to curvature of the flow. For simplicity, let $\Omega = m + n$y , then

$$\rho \frac{\partial H(\bar{u}\,\bar{v})_d}{\partial y} + 2\rho \int_0^H \left(\frac{\bar{u}\,\bar{v}}{r} + \frac{\overline{u'v'}}{r} \right) dz = \Omega \qquad (13)$$

Further discussion on this assumption is given later. Combining Eqs. (11) and (12) gives

$$\rho g H S_o + \frac{\partial H \bar{\tau}_{yx}}{\partial y} - \tau_b \sqrt{1 + \frac{1}{ss^2}} = m + ny \qquad (14)$$

Through Eq. (8) and the following assumptions (15),

$$\tau_b = \left(\frac{f}{8}\right) \rho U_d^2 \; ; \; \bar{\tau}_{yx} = \rho \bar{\varepsilon}_{yx} \frac{\partial U_d}{\partial y} \; ; \; \bar{\varepsilon}_{yx} = \lambda U_* H \qquad (15)$$

where U_* = shear velocity [= $(\tau_b/\rho)^{1/2}$], Eq. (14) can be rewritten as

$$\rho g H S_o - \rho \frac{f}{8} U_d^2 \left(1 + \frac{1}{ss^2}\right)^{1/2} + \frac{\partial}{\partial y}\left\{ \rho \lambda H^2 \left(\frac{f}{8}\right)^{1/2} U_d \frac{\partial U_d}{\partial y} \right\} = m + ny \qquad (16)$$

where f = Darcy-Weisbach friction factor, and λ = dimensionless eddy viscosity.

For given coefficients (f, λ, m and n), Eq.(16) becomes a constant coefficient ordinary differential equation for the velocity variable (U_d^2) with respect to the lateral distance (y). An analytical solution to Eq.(16) can be obtained as follows (Tang & Knight, 2008a):

<1>For a domain of constant depth:

$$U_d = (A_1 e^{\gamma y} + A_2 e^{-\gamma y} + k)^{1/2} \qquad (17)$$

$$k = \frac{8 g S_o H}{f} - \frac{8}{\rho f}(m + ny) \; ; \; \gamma = \sqrt{\frac{2}{\lambda}} \left(\frac{f}{8}\right)^{1/4} \frac{1}{H} \qquad (18)$$

<2> For a domain with linearly varying bed (1:ss):

$$U_d = \left(A_3 \xi^{\alpha} + A_4 \xi^{-(\alpha+1)} + \omega \xi + \eta\right)^{1/2} \qquad (19)$$

192 $$\alpha = -\frac{1}{2} + \frac{1}{2}\sqrt{1 + \frac{ss\sqrt{1+ss^2}}{\lambda}\sqrt{8f}};\quad \omega = \frac{gS_o + n\,ss/\rho}{\frac{\sqrt{1+ss^2}}{ss}\left(\frac{f}{8}\right) - \frac{\lambda}{ss^2}\sqrt{f/8}};\quad \eta = \frac{-(m + Hn\,ss)}{\rho\sqrt{1+\frac{1}{ss^2}}\left(\frac{f}{8}\right)} \quad (20)$$

193

194 in which A_1-A_4 are unknown constants, and ξ is the local depth given by ξ =H -y /ss (for y>0).

195

196 **Validation of secondary flow term in the new model**

197

198 The proposed approximation for the secondary flow and additional Reynolds stress due to curvature
199 [RHS of Eq.(11)] is in the form of Eq.12. Many experimental researches have been undertaken on
200 flows in river bends, but the majority of measurements have only focused on streamwise and lateral
201 velocities. There is little data available on 3D flow velocities and stresses. Booij (2003) investigated
202 the secondary flow in a 180° rectangular bend flume by undertaking detailed measurement of 3D
203 velocities using a 3D LDV system. Such a valuable data set enables one to evaluate both the
204 secondary flow and the additional Reynolds stress terms in a curved channel, i.e. all the terms on the
205 RHS of Eq. (11). The cross-section of the 0.5m wide flume was rectangular and the radius of
206 curvature of the centre of flume was 4.10m, as shown in Fig. 3. The flow depth was set at 0.052m
207 for this particular series of experiments.

208

209 Two detailed data sets, at two cross-sections 29° and 135° from the entrance of flume, are given by
210 van Balen *et al*. (2009), and are repeated in Fig.4. The flow at the 135° cross-section was found to be
211 fully developed, and therefore this set of data was used to evaluate the secondary flow and the
212 additional Reynolds stress terms in Eq. (20).

213

214 To validate the approximate expression in Eq. (12), each term on the left side of Eq. (12) has been
215 evaluated from the data extracted from Fig.4 (after van Balen et al., 2009). The results are analysed
216 and given by Figures 5-7. Fig.5 shows an approximately linear variation of the secondary flow term
217 $\rho H(\overline{u}\,\overline{v})_d$ from inner (left) to outer (right) side along the cross section of channel with a maximum
218 located slight towards the left of the central line. A similar approximately linear variation of the
219 additional Reynolds stress term, $2\rho\int_0^H\left(\frac{\overline{u}\,\overline{v}}{r} + \frac{\overline{u'v'}}{r}\right)dz$, is given in Fig.6. The corresponding total
220 additional secondary flow term, $\rho H(\overline{u}\,\overline{v})_d + 2\rho\int_0^H\left(\frac{\overline{u}\,\overline{v}}{r} + \frac{\overline{u'v'}}{r}\right)dz$, termed as Ω for convenience as
221 shown in Eq. (13), is given in Fig.7, which clearly demonstrates an approximate bilinear transverse
222 distribution of the total additional secondary flow term (RHS of Eq. 11). Therefore, the

approximation given by Eq. (12) appears to be reasonable. In the next section we analyze how the coefficients (*m*,*n*) affect the predicted distributions.

Discussion of Results

In order to model the lateral distribution of depth-averaged velocity, as shown by Eqs. (17) and (19), four parameters (f, λ; *m* and *n*) are needed, where m and n represents the total additional flow term in a curved channel, expressed as the right side Ω of Eq.(11). The parameters (*f*, λ, Γ), where Γ is the secondary flow term defined as $\rho \frac{\partial H(\overline{u}\,\overline{v})_d}{\partial y}$, have been studied extensively for different cases in straight channels by Shiono & Knight (1991), Abril & Knight (2004), McGahey (2006), McGahey *et al*. (2006), Chlebek & Knight (2006), Knight *et al*.(2007, 2010a&b) and Tang & Knight (2008a,b). They found the model was less sensitive to λ for overbank flows than for inbank flows, and that even constant values of *f*, λ and Γ in particular panels or zones (groups of panels) may give satisfactory results. In the following section, the influence of Ω on the lateral distribution of velocity is discussed, using modelling results for curved rectangular channels with a flat bed.

Boundary Conditions for solution of U_d

For the channel shown in Fig.8, the cross-section may be divided into several panels (*i*) with either constant depth or linear depth domains, where the analytical solutions of U_d given by (17) and (19) apply respectively. Two unknown constants A_1 and A_2 (Eq. 17) or A_3 and A_4 (Eq. 19) in each domain can be obtained using appropriate boundary conditions as follows (see Fig.8):

- The no-slip condition, i.e. U_d =0 at the remote boundaries;
- The continuity of the velocity U_d at each domain junction, i.e. $U_d^{(i)} = U_d^{(i+1)}$ at y=b;
- The continuity of unit force ($H\overline{\tau}_{yx}$) at each domain junction, i.e. $[H\overline{\tau}_{yx}]^{(i)} = [H\overline{\tau}_{yx}]^{(i+1)}$ at y=b.

It follows using (16) for a continuous depth domain that the continuity of unit force at each junction is as given by (Tang and Knight, 2008b):

$$\left(\mu \frac{\partial U_d}{\partial y}\right)^{(i)} = \left(\mu \frac{\partial U_d}{\partial y}\right)^{(i+1)} \text{ with } \mu = \lambda\sqrt{f} \qquad (21)$$

where *i* is panel number.

Modelling philosophy and calibration coefficients

The philosophy adopted in the analytical solutions (17) & (19) is based on a constant value for (*m*, *n*) used to determine the distribution of Ω for each panel, whether the panel has a flat bed or a linearly varying sloping bed. The cross-section of the channel can normally be split into a number of panels in which the calibration parameters are held constant. Generally panel boundaries are chosen where the flow depth is discontinuous or changes. In those cases characterized by complex secondary flow cells, further division of the channel may be required. More details about how to divide the channel according to the size and distribution of secondary cells is given by Knight *et al*. (2007). The friction factor in each panel is normally assumed to be constant, based on experimental results and by using the back calculated values from Darcy-Weisbach equation. To simplify the calibration procedure, and to make the work of the modeller easier, a constant 'standard' value for λ for most panels (λ = 0.07) is assumed.

Modelling results for a curved rectangular channel

This session examines the impact of the total additional secondary flow term (Ω) on the lateral velocity distribution using the model in a smooth curved rectangular channel similar to that used in the flume experiments by Booij (2003). The channel bed slope is set at 0.0001, and the channel width is 0.50m with various curvature radius r, as shown in Fig. 9, where y is towards outside bank of the channel, B = channel width, H = flow depth, and b1 and b2 are the panel widths respectively for panels (1) and (2). For all cases values of ρ =1000 kg/m^3 and g =9.807 m/s^2 were adopted.

In the modelling, *f* = 0.010 was used for the smooth channel, and the total additional secondary flow term Ω (= *m* + *n*y) is assumed to be bi-linearly distributed over the channel width, with Ω = 0 at the edge of channel, implying that *m* = 0 in panel (1). To test how the *n* value and the ratio of b1/B (B=b1+b2) affect the velocity distribution, some results are shown in Figs. 10-11, along with the experimental data by Booij (2003).

Fig.10 shows that the velocity decreases as *n* increases, and the velocity distribution is symmetric as expected due to the two equal width panels used for the same *n*-value. It also shows that the results using *n* =0.02 agree with the data reasonably well, and that the results without secondary flow overestimate slightly, as it is not surprising for the mild curved channel (R/B = 8.2).

As the data reveal that the secondary cells are not symmetric, we examined how the panel size (corresponding to the secondary cell distribution) affects the velocity distribution. The modelled results with varying b1/B ratios are shown in Fig.11, which demonstrates that the velocity distribution is skewed towards the inside bank as the maximum secondary flow location changes from 30% to 70% of whole channel width away to the inner bank.

However, the value of m ($\Omega = m + n\mathrm{y}$) at the two banks of a channel is unlikely to be zero in most cases. This can be explained as follows: although the velocity components (u,v) at the edge of a channel are zero, the data for $\rho \mathrm{H}(\overline{\mathrm{u}}\,\overline{\mathrm{v}})_{\mathrm{d}}$ show that it varies approximately linearly over the majority of the channel, except at the extreme edges. Therefore the gradient of $\rho \mathrm{H}(\overline{\mathrm{u}}\,\overline{\mathrm{v}})_{\mathrm{d}}$ is not zero at these extreme points, but has a limiting small value. To further explore how the values of (m, n) affect the velocity distribution, a comparison of the results with varying m_1 (value of m in panel 1) is given in Fig. 12, whereas Fig.13 shows results of velocity distribution for varying m_2 (value of m in panel 2). In the modelling, the same channel was used with b1/B = 50%. Fig.12 shows that m_1 has a significant impact on the velocity distribution, and the velocity decreases as m_1 increases, which results in a skewed distribution of velocity. Fig.13 shows m_2 has a similar impact to m_1. This demonstrates that the model is capable of predicting the lateral distribution of velocity using appropriate values for m_1 and m_2.

Conclusions

Based on a RANS approach and the assumption of a bi-linear distribution for the additional secondary flow terms, an analytical model is proposed that predicts the lateral distribution of depth-averaged velocity of flow in curved open channels. The two parameters (m, n) for the total additional secondary flow term, Ω (=m+ny), have been examined for their impacts on the velocity distribution for typical case in a rectangular channel with flat bed. The following conclusions may be drawn:

1) The additional flow term (Ω) can be approximated by a linear variation with lateral distance, as given by Eqs. (12) and (13). This has been validated using the limited data that are available.

2) Based on the premise of point (1) the two analytical solutions for U_d, given by Eqs. (17) and (19), are shown to describe the lateral distribution of depth-averaged velocity in a curved rectangular channel for a flat bed and a sloping side bed respectively.

3) It is demonstrated that the modelled results agree reasonably well with the limited experimental data.

4) Model tests for a curved rectangular channel with flat bed show that m values have a significant influence on the results, as shown by Figs. 12 & 13. By contrast, n values have a relatively small impact on the results, as shown by Figs. 10 & 11.

5) Although the model is capable of predicting the lateral distribution of depth-averaged velocity, further experimental work is needed to valid the m and n values and to define the number and

position of the dominant secondary flow cells in bends with different geometries.

Notation:

$\bar{\varepsilon}_{yx}$ = depth-averaged eddy viscosity, defined by (15);

{*u,v,w*} = velocity components in the coordinates {s,n,z} or {*x,y.z*} directions;

A_1 to A_4 = constants in (17) and (19);

B = bed width of channel;

b_1 , b_2 = panel width of channel ;

f = Darcy-Weisbach friction factor, defined by (15);

g = gravitational acceleration;

H = flow depth in channel;

k = coefficient constant, defined by (18);

ss = channel side slope (1:ss, vertical : horizontal);

S_o = channel bed slope;

U_* = shear velocity [= $(\tau_b/\rho)^{1/2}$];

U_d = depth-averaged streamwise velocity, defined by (8);

x = streamwise co-ordinate;

y = lateral co-ordinate;

z = co-ordinate normal to bed;

λ = dimensionless eddy viscosity, defined by (15);

ρ = fluid density;

Ω = transverse gradient of secondary flow term, defined by (13);

α = coefficients in (19);

γ = coefficient constants, defined by (18);

η = coefficients in (30);

μ = coefficient, defined by (21)

τ_b = local boundary shear stress, defined by (15);

ω = coefficients in (20);

Acknowledgments

The works are supported by the open funds provided by the State Key Lab of Hydraulics and Mountain River Engineering at Sichuan University, China (SKLH-OF-0906).

References

Abril, J.B. and Knight, D.W. (2004). "Stage-discharge prediction for rivers in flood applying a depth-averaged model." *Journal of Hydraulic Research,* IAHR, 42(6), 616-629.

Albayrak, I. and Lemmin, U. (2011). Secondary currents and corresponding surface velocity patterns in a turbulent open-channel flow over a rough bed. Journal of Hydraulic Engineering, 137(11), 1318-1334.

Ascanio, M. F. and Kennedy, J. F. (1983). Flow in alluvial-river curves. J. of Fluid Mechanics, 133, 16.

Blanckaert, K. & de Vriend, H. J. (2005). Turbulence structures in sharp open-channel bends. J. of Fluid Mechanics, 536, 27-48.

Blanckaert, K. (2001). Discussion of Bend-flow simulation using 2D depth averaged model, ASCE, Journal of Hydraulic Engineering, 127(2), 167-170.

Blanckaert, K. (2005). Discussion of Investigation on the Stability of Two-Dimensional Depth-Averaged Models for Bend-Flow Simulation. ASCE, Journal of Hydraulic Engineering, 131(7), 625-628.

Blanckaert, K. and Graf, W. H. (2001). Mean flow and turbulence in open-channel bend. ASCE, Journal of Hydraulic Engineering, Vol. (127), No. 10, 835-847.

Blanckaert, K. and Graf, W. H. (2004). Momentum Transport in Sharp Open-Channel Bends. ASCE, Journal of Hydraulic Engineering, Vol. (130), No. 3, 186-198.

Blanckaert, K. and H. J. de Vriend (2003), Nonlinear Modeling of Mean Flow Redistribution in Curved Open Channels, Water Resources Research, 39 (12), doi:10.1029/2003WR002068.

Blanckaert, K. and H. J. de Vriend (2010), Meander dynamics: A nonlinear model without curvature restrictions for flow in open-channel bends, J. of Geophysical Research, 115, F04011.

Blanckaert, K., Buschman, F. A., Schielen, R and Wijbenga, J. H. A. (2008). Redistribution of Velocity and Bed-Shear Stress in Straight and Curved Open Channels by Means of a Bubble Screen: Laboratory Experiments. ASCE, Journal of Hydraulic Engineering, 134(2), 184-195.

Booij, R. (2002). Modelling of the secondary flow structure in river bends. River Flow 2002, Sweets & Zitlinger, Lisse [Eds Bousmar and Zech], 127-133.

Booij, R. (2003). Measurements and large-eddy simulations of the flows in some curved flumes. J. Turbulence 4, 1–17.Modelling the flow in curved tidal channels and rivers. International conference on Estuaries and Coasts. November 9-11, 2003, Hangzhou, China, 786-794.

Booij, R. (2004). Negative eddy viscosity in river bends. River Flow 2004, Proc. 2nd Int. Conf. on Fluvial Hydraulics, 23-25 June, Napoli, Italy [Eds M. Greco, A. Carravetta & R.D. Morte], 307-315.

Camporeale, C., P. Perona, A. Porporato, and L. Ridolfi (2007), Hierarchy of models for meandering rivers and related morphodynamic processes, Reviews of Geophysics, 45 (1).

Chang, H.H. (1998). Fluvial Processes in River Engineering, Krieger Publishing Company, Malabar, Florida.

Chlebek, J. and Knight, D.W. (2006). A new perspective on sidewall correction procedures, based on SKM modelling , RiverFlow 2006, Lisbon, Vol. 1, [Eds Ferreira, Alves, Leal & Cardoso], Taylor & Francis, 135-144.

Constantinescu, G., M. Koken, and J. Zeng (2011), The structure of turbulent flow in an open channel bend of strong curvature with deformed bed: Insight provided by detached eddy simulation, Water Resources Research, 47, W05515.

Constantinescu, G., S. Kashyap, T. Tokyay, C. D. Rennie and R. D. Townsend (2013), Hydrodynamic processes and sediment erosion mechanisms in an open channel bend of strong curvature with deformed bathymetry, J. of Geophysical Research – Earth Surface, 118, 1-17.

Engelund, F. (1974). Flow and Bed Topography in Channel Bends. J. of the Hydraulics Division, ASCE, 100(HY11):1631-1648.

Ervine, D. A., Babaeyan-Koopaei, K. and Sellin, R. H. J. (2000). Two-dimensional solution for straight and meandering overbank flows. Journal of Hydraulic Engineering, 126(9), 653-669.

Hsieh, T. Y. and Yang, J. C. (2003). Investigation on the Suitability of Two-Dimensional Depth-Averaged Models for Bend-Flow Simulation. Journal of Hydraulic Engineering, 129(8), 597-612.

Jamieson, E. C., G. Post, and C. D. Rennie (2010), Spatial variability of three-dimensional Reynolds stresses in a developing channel bend, Earth Surf. Processes Landforms, 35, 1029–1043.

Jamieson, E., Rennie, C., and Townsend, R. (2013). ”Turbulence and Vorticity in a Laboratory Channel Bend at Equilibrium Clear-Water Scour with and without Stream Barbs.” *J. of Hydraulic Engineering*, 139(3), 259–268.

Jin, Y.C. and Steffler, P.M. (1993). Predicting Flow in Curved Open Channels by Depth-Averaged Method. Journal of Hydraulic Engineering, 119(1): 109-124.

Johannesson, H. and Parker G. (1989). Velocity redistribution in meandering rivers. Journal of Hydraulic Engineering, 115 (8), 1019– 1039.

Kashyap,I, Constantinescu, G, Rennie, C. D, Post, G, and Townsend R. (2012), Influence of Channel Aspect Ratio and Curvature on Flow, Secondary Circulation, and Bed Shear Stress in a Rectangular Channel Bend, Journal of Hydraulic Engineering, 138, 12, 1045-1059.

Khan, A.A. and Steffler, P.M. (1996). Vertically averaged and moment equations model for flow over curved beds. Journal of Hydraulic Engineering, 122(1):3-9.

Knight D.W. (2012). Hydraulic Problems in Flooding: from Data to Theory and from Theory to Practice, in *Experimental and Computational Solutions of Hydraulic Problems* [Ed P Rowinski], International School of Hydraulics, Lochow, Poland, May 2012, Springer, 1-34.

418 Knight, D.W., and Sellin, R.H.J. (1987). The SERC Flood Channel Facility. Journal of the Institution of
419 Water and Environmental Management, London, 1(2), Oct., 198-204.
420 Knight, D.W., Mc Gahey, C., Lamb, R. & Samuels, P.G. (2010b). *Practical Channel Hydraulics –*
421 *Roughness, Conveyance and Afflux*, CRC Press/Taylor & Francis, 1-354.
422 Knight, D.W., Omran, M. and Tang, X. (2007). Modelling depth-averaged velocity and boundary
423 shear in trapezoidal channels with secondary flows, Journal of Hydraulic Engineering, ASCE, Vol.
424 133, No. 1, January, pp. 39-47.
425 Knight, D.W., Tang, X., Sterling, M., Shiono, K. & Mc Gahey, C. (2010a). Solving open channel flow
426 problems with a simple lateral distribution model, *Riverflow 2010*, Proceedings of the Int. Conf. on
427 Fluvial Hydraulics, [Eds A. Dittrich, K. Koll, J. Aberle, and P. Geisenhainer], Braunschweig,
428 Germany, Sept. 8-10, Bundesanstalt fur Wasserbau (BAW), Karlsruhe, Germany, Keynote address,
429 Vol I, 41-48.
430 Mc Gahey, C. (2006). A practical approach to estimating the flow capacity of rivers, PhD Thesis,
431 Faculty of Technology, The Open University (and British library), May, 1-371.
432 Mc Gahey, C., Knight, D.W. & Samuels, P.G. (2009). Advice, methods and tools for estimating
433 channel roughness, Water Management, Proc. of the Instn of Civil Engineers, London, Vol. 162,
434 Issue WM6, Dec., 353-362.
435 Nezu I, Tominaga A, Nakagawa H. Field measurements of secondary currents in straight rivers. J. of
436 Hydraulic Engineering,119(5),598–614
437 Ottevanger, W., Blanckaert, K., W.S.J. Uijttewaal, and H.J. de Vriend (2013), Meander dynamics: A
438 reduced order non-linear model without curvature restrictions for flow and bed morphology, J. of
439 Geophysical Research – Earth Surface, doi: 10.1002/jgrf.20080.
440 Rozovskii, J.L. (1957). Flow of water in bends of open channel. Academic of Science of the Ukrainian
441 SSR, Kiev.
442 Schlichting, H. (1979). Boundary-layer theory, 7th Ed., McGraw-Hill,New York.
443 Sharifi, S. and Sterling, M. (2009). A novel application of a multi-objective evolutionary algorithm in
444 open channel flow modelling, Journal of Hydroinformatics, IWA Publishing, 11.1, 31-50.
445 Shiono, K., and Knight, D.W. (1991). "Turbulent open channel flows with variable depth across the
446 channel." *Journal of Fluid Mechanics*, 222, 617-646 (and Vol. 231, Oct., 693).
447 Stoesser, T., N. Ruether, and N. R. B. Olsen (2010), Calculation of primary and secondary flow and
448 boundary shear stresses in a meandering channel, Adv. Water Resources., 33(2), 158–170,
449 doi:10.1016/j.advwatres.2009.11.001.
450 Sukhodolov AN. (2012). Structure of turbulent flow in a meander bend of a lowland river. Water
451 Resources Research ,48: W01516.

Tang, X. and Knight D.W. (2008a). "A General Model of Lateral Depth-Averaged Velocity Distributions for Open Channel Flows", Advances in Water Resources, 31(5), pp 846-857.

Tang, X. and Knight, D W (2008b). Lateral depth-averaged velocity distribution and bed shear in rectangular compound channels, *Journal of Hydraulic Engineering*, 134(9), 1337-1342.

Tang, X. and Knight, D W (2009). Analytical models for velocity distributions in Open Channel Flows", *Journal of Hydraulic Research,* 47(4), 418-428.

van Balen W., Uijttewaal, W. S. J and Blanckaert, K (2009). Large-eddy simulation of a mildly curved open-channel flow. Journal of Fluid Mechanics. Vol. 630, 413-442.

Yalin, M.S. (1992). River Mechanics. Pergamon Press, Oxford, New York.

Yeh, K.C. and Kennedy, J.F. (1993). Moment Model of Nonuniform Channel-Bed Flow. I: Fixed Beds. Journal of Hydraulic Engineering, 119(7): 776-795.

List of Figures:

Fig.1. A typical flow structure in a bend (modified after Balen et al. 2009)

Fig.2. A sketch of a cross-section in a bend with secondary flow cells

Fig. 3. Curved experimental flume (after Booij,2003)

Fig. 4. Velocity components from the experiments at locations equidistantly placed from the inner bank (left) to the outerbank (right) for the 135^{o}cross-section. Vav =0.2ms^{-1} (after Balen et al. 2009).

Fig. 5. The lateral distribution of secondary flow term, $\rho \mathrm{H}(\overline{\mathrm{u}}\,\overline{\mathrm{v}})_{\mathrm{d}}$ versus y (m)

Fig. 6 . The lateral distribution of additional secondary flow term, $2\rho \int_0^{\mathrm{H}} \left(\frac{\overline{\mathrm{u}}\,\overline{\mathrm{v}}}{\mathrm{r}} + \frac{\overline{\mathrm{u'v'}}}{\mathrm{r}}\right) \mathrm{dz}$ versus y (m)

Fig. 7. The lateral distribution of total additional flow term, $\rho \mathrm{H}(\overline{\mathrm{u}}\,\overline{\mathrm{v}})_{\mathrm{d}} + 2\rho \int_0^{\mathrm{H}} \left(\frac{\overline{\mathrm{u}}\,\overline{\mathrm{v}}}{\mathrm{r}} + \frac{\overline{\mathrm{u'v'}}}{\mathrm{r}}\right) \mathrm{dz}$

Fig.8. Sketch of a channel with two panels

Fig. 9 A sketch of a rectangular cross-section

Fig.10 Result of modelled depth-averaged velocity for various n values (H = 0.052m)

Fig.11 Modelled depth-averaged velocity for two panels with various ratio of b1/B (n =0.02)

Fig.12 Modelled depth-averaged velocity with varying m_1 values in panel 1

Fig.13 Modelled depth-averaged velocity with varying m_2 values in panel 2

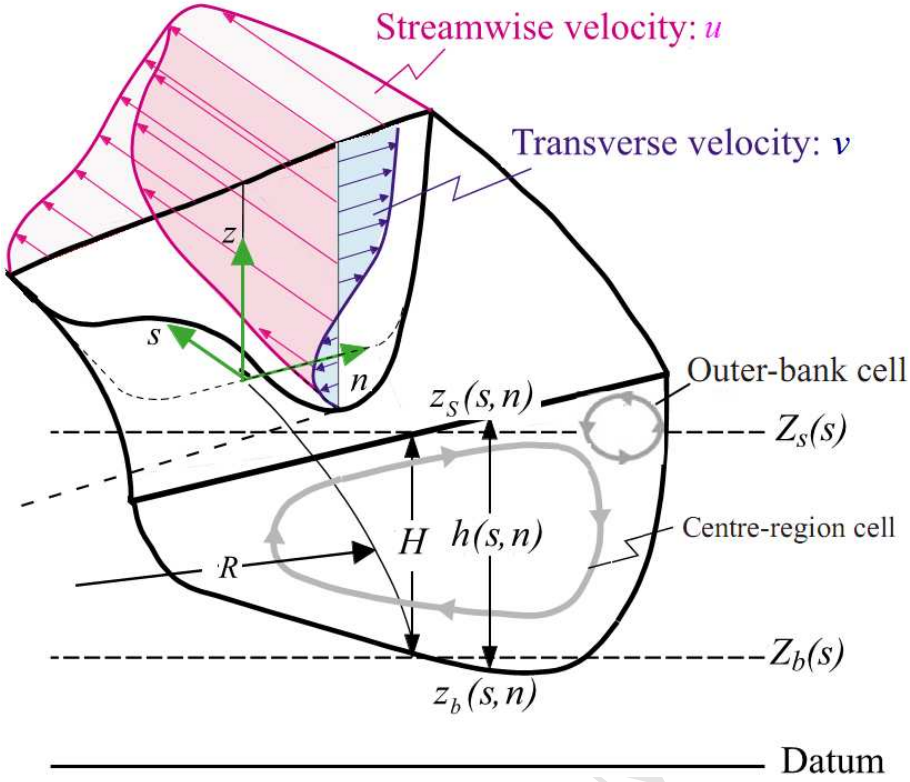

Fig.1. A typical flow structure in a bend (modified after Blanckaert & de Vriend, 2010)

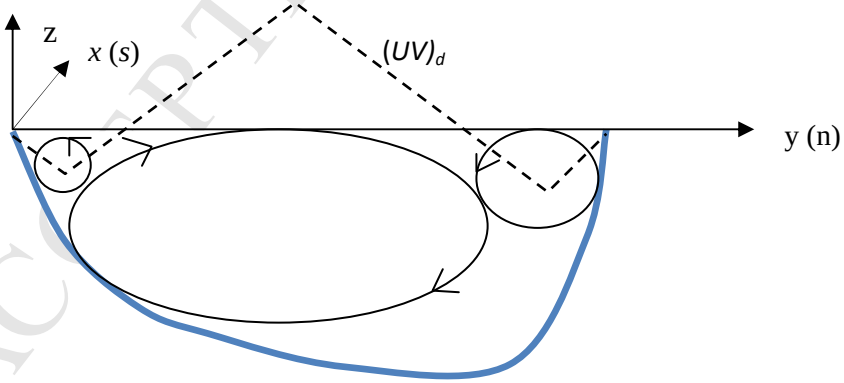

Fig.2. A sketch of a cross-section in a bend with secondary flow cells, where a flat surface is assumed as simplicity.

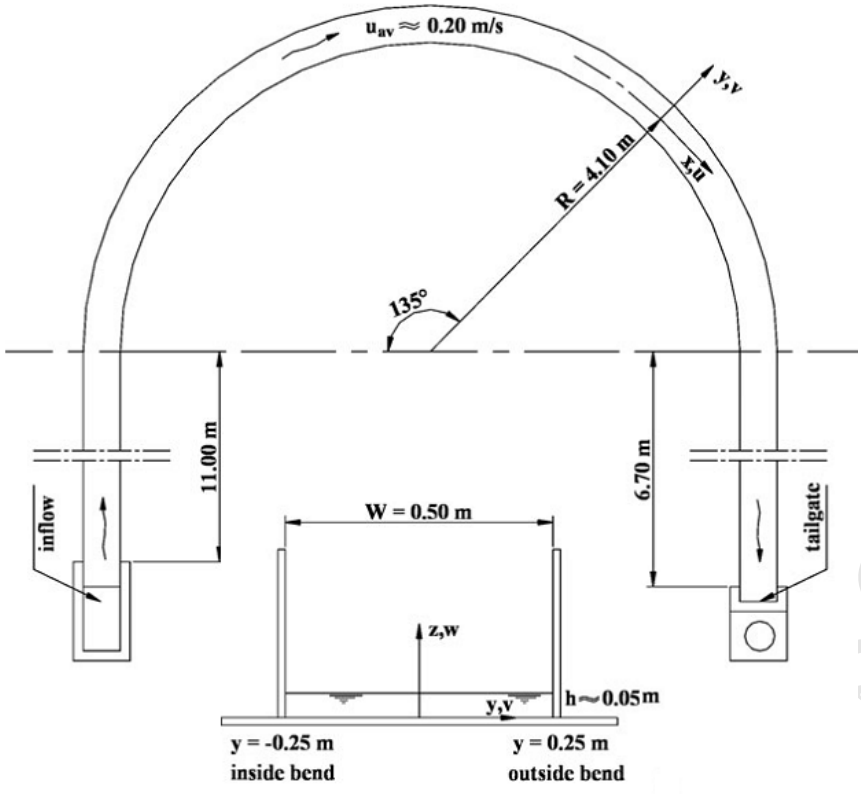

Fig. 3. Curved experimental flume (after Booij,2003)

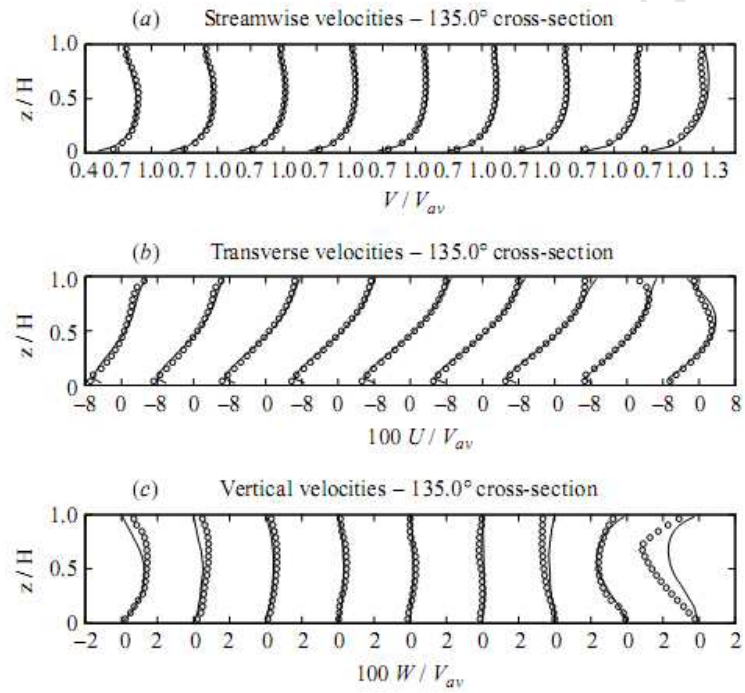

Fig. 4. Velocity components from the experiments at locations equidistantly placed from the inner bank (left) to the outerbank (right) for the 135°cross-section. Vav =0.2ms^{-1} (after van Balen et al. 2009), where the circle symbols are measured data and the solid line denotes the model of van Balen et al.

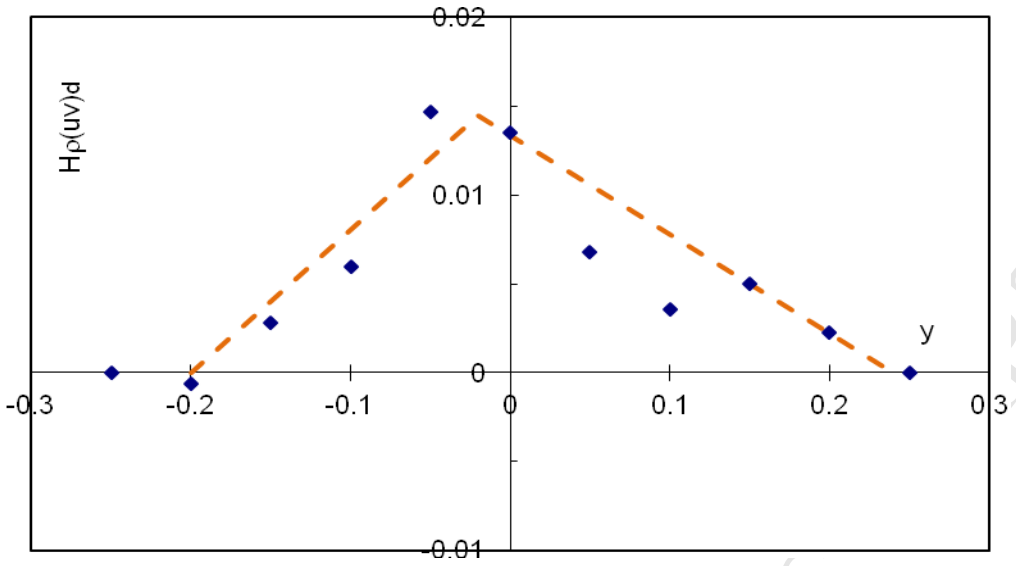

Fig. 5 The lateral distribution of secondary flow term, $\rho H(\overline{u}\,\overline{v})_d$ versus y (m), where y varies from inner (left) to outer (right) side of channel and the symbols denote the data from van Balen et al.(2009)

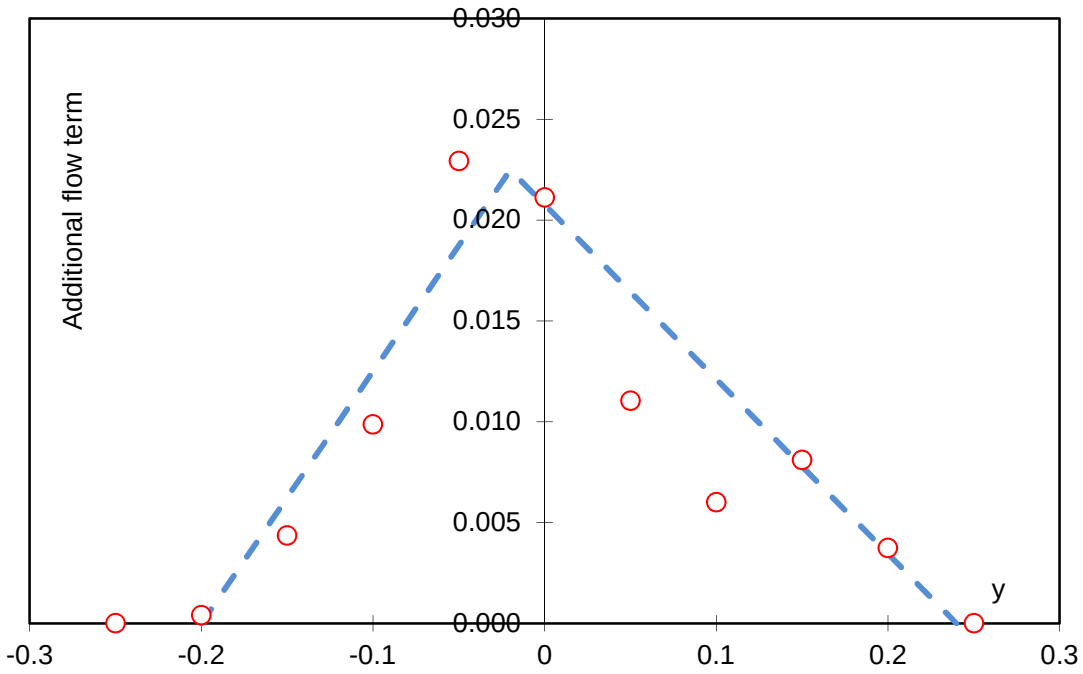

Fig. 6 The lateral distribution of additional secondary flow term, $2\rho\int_0^H\left(\frac{\overline{u}\,\overline{v}}{r}+\frac{\overline{u'v'}}{r}\right)dz$ versus y (m), where y varies from inner (left) to outer (right) side of channel and the circles denote the data from van Balen et al.(2009)

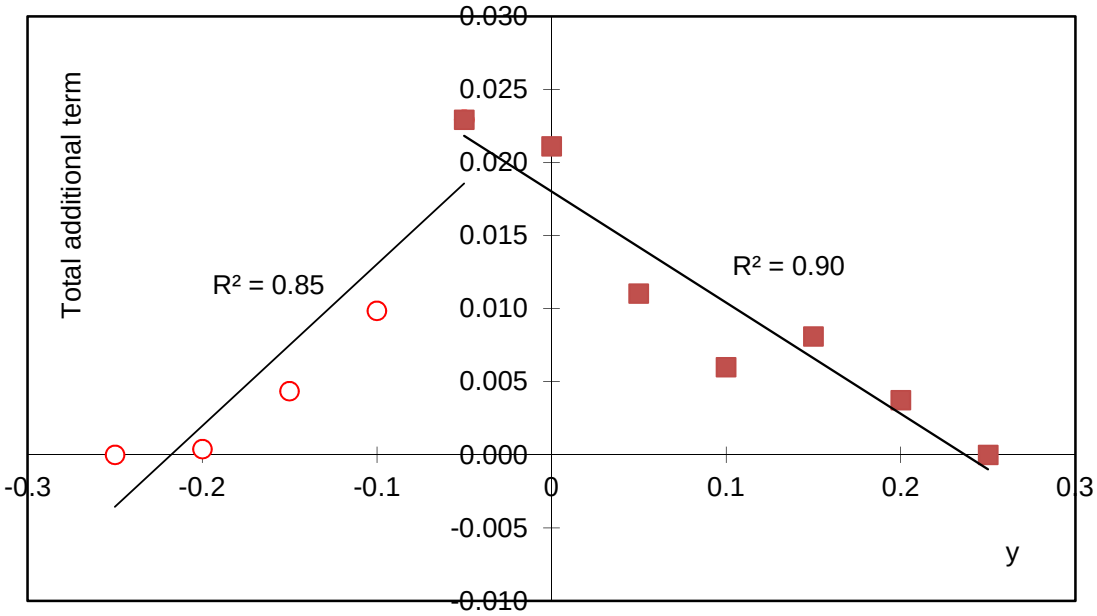

Fig. 7. The lateral distribution of total additional flow term, $\rho H(\overline{u}\,\overline{v})_d + 2\rho \int_0^H \left(\frac{\overline{u}\,\overline{v}}{r} + \frac{\overline{u'v'}}{r}\right) dz$, where the symbols denote the data from van Balen et al.(2009)

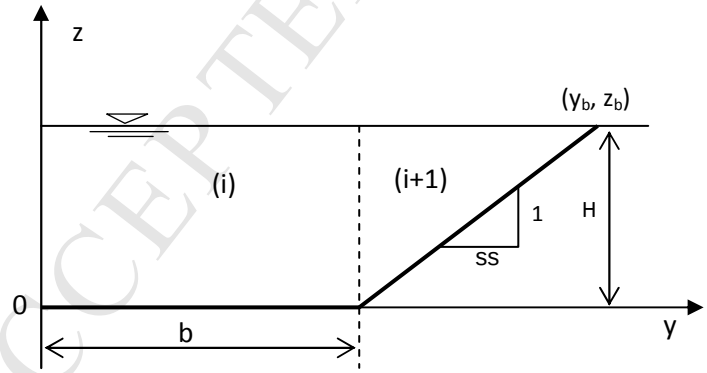

Fig.8 Sketch of a channel with two panels

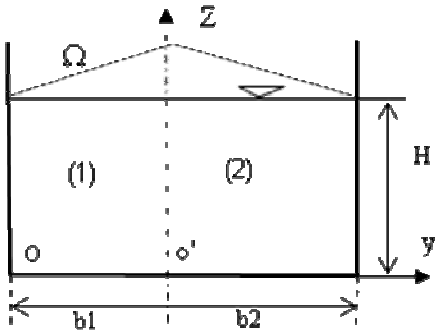

Fig. 9 A sketch of a rectangular cross-section

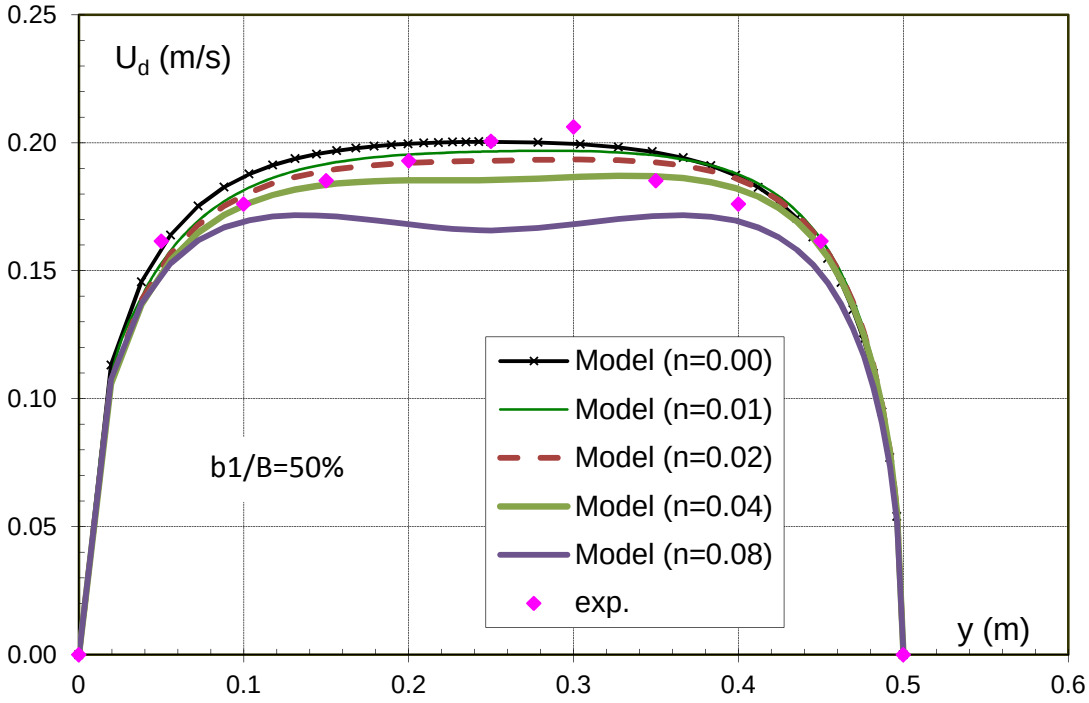

Fig.10 Result of modelled depth-averaged velocity for various n values (m=0, H = 0.052m)

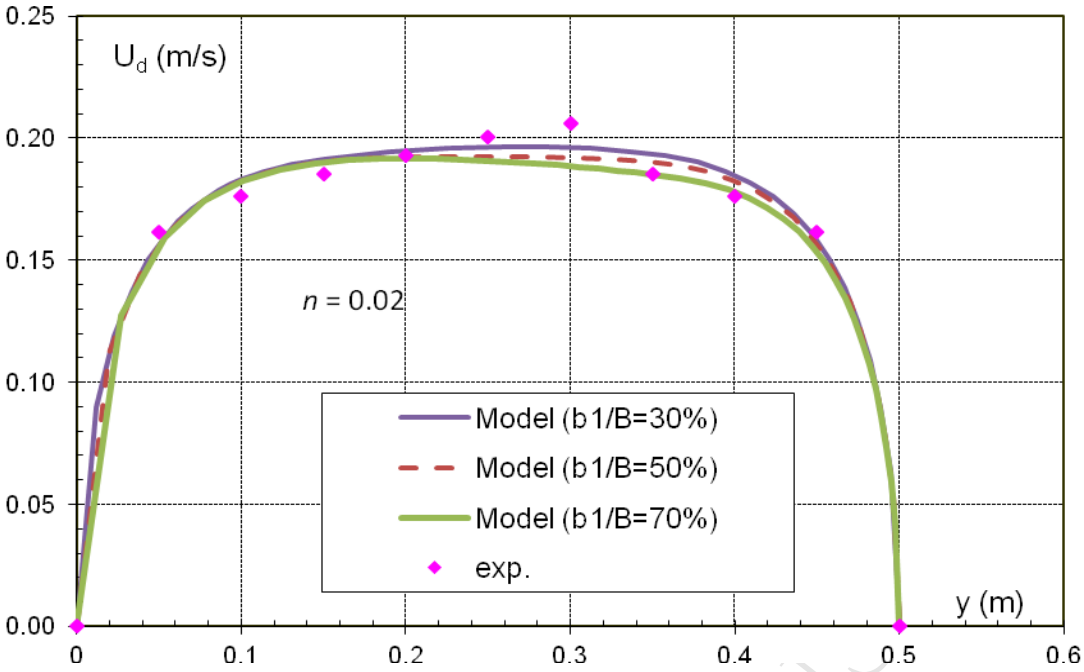

Fig.11 Modelled depth-averaged velocity for two panels with various ratio of b1/B (n =0.02, m=0)

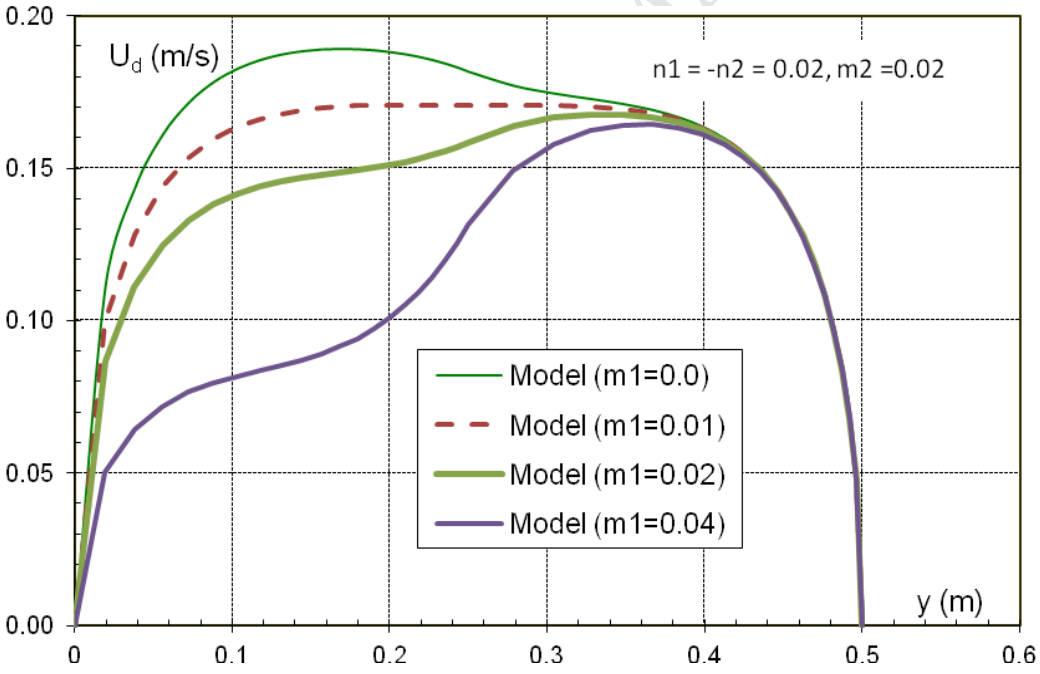

Fig.12 Modelled depth-averaged velocity with varying m_1 values in panel 1

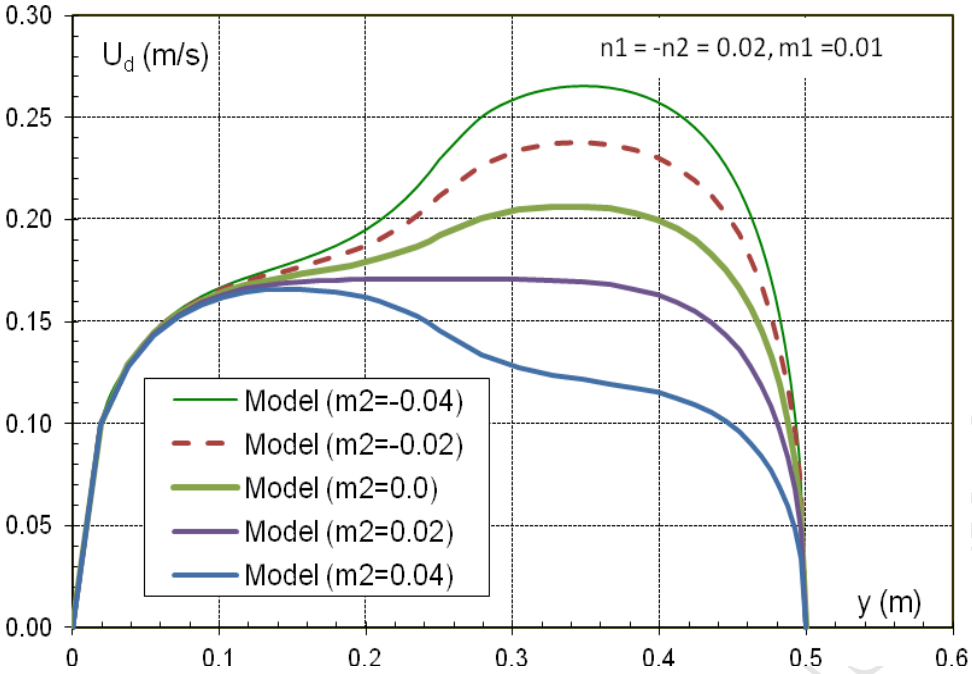

Fig.13 Modelled depth-averaged velocity with varying m_2 values in panel 2

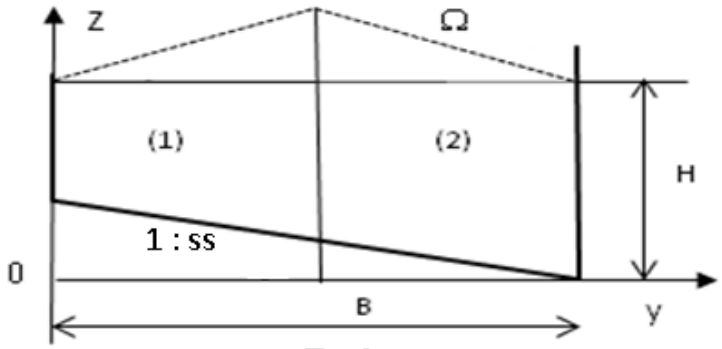

Fig. 14 Sketch of a curved rectangular channel with transverse sloping bed

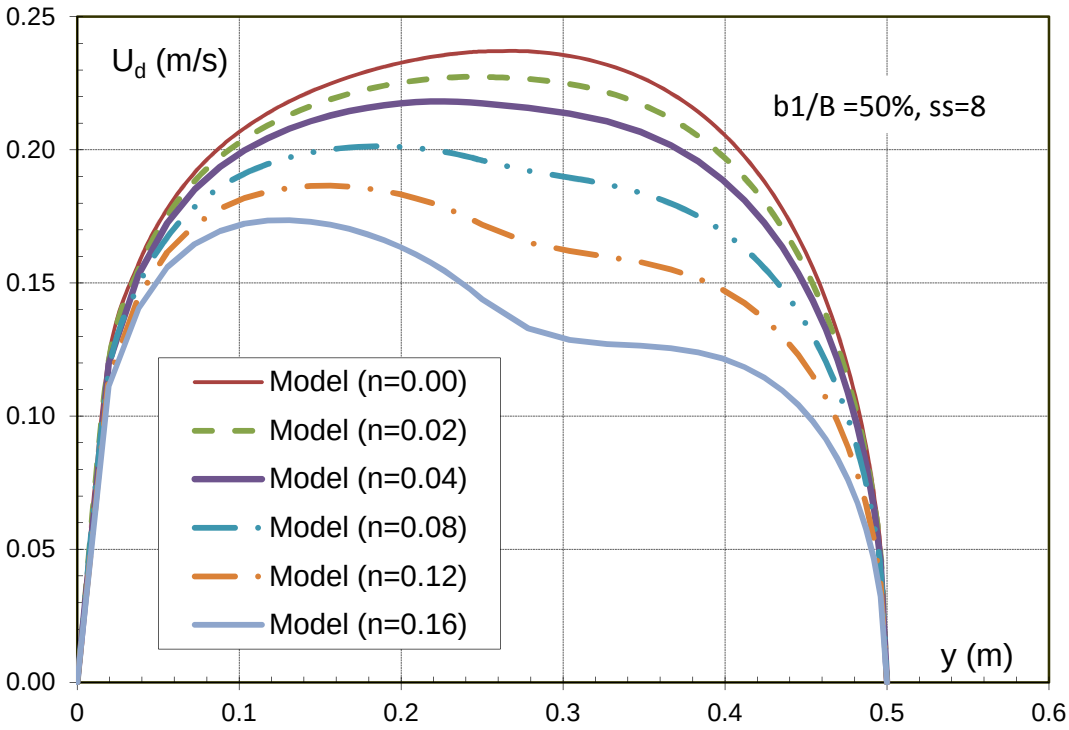

Fig.15 Modelled depth-averaged velocity with varying n values

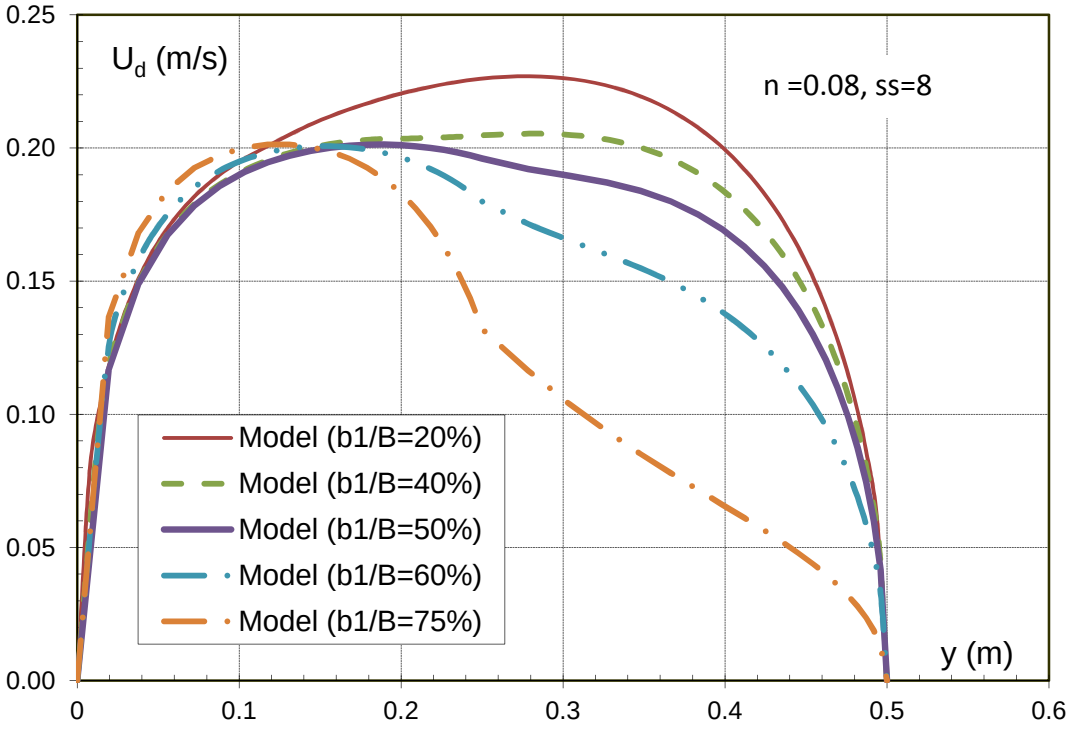

Fig.16 Modelled depth-averaged velocity with varying ratios of b/B

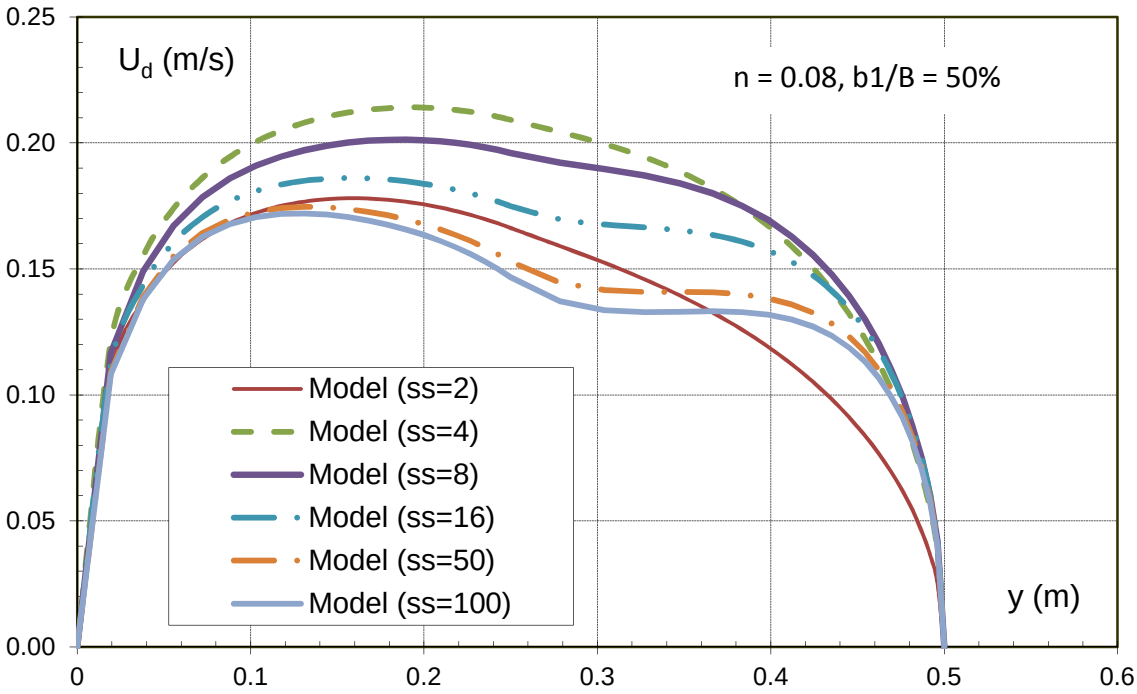

Fig.17 Modelled depth-averaged velocity with varying bed side slope ss values